



Synthetic 3-alkylpyridine alkaloid analogues as a new scaffold against leukemic cell lines: cytotoxic evaluation and mode of action

Fernanda Cristina Gontijo Evangelista¹ · Aline de Freitas Lopes² · Silmara Nunes Andrade² · Camila de Souza Barbosa² · Julia Dias da Silva² · Alessandra Mirtes Marques Neves² · Cristina de Mello Gomide Loures¹ · Larissa Froede Brito¹ · Lirlândia Pires de Sousa¹ · Karina Braga Gomes Borges¹ · Gustavo Henrique Ribeiro Viana² · Fernando de Pilla Varotti² · Adriano de Paula Sabino¹

Received: 15 May 2019 / Accepted: 6 July 2019 / Published online: 19 July 2019
© Springer Science+Business Media, LLC, part of Springer Nature 2019

Abstract

Leukemia is a malignant disease that originates in the bone marrow, local of blood cells production. Chemotherapy treatment is one of the alternatives to improve the survival of patients. In this context, the search for new compounds with potential cytotoxic action is justified. The present work evaluated the cytotoxic activity of 16 new synthetic analogs of 3-alkylpyridine alkaloids. The cytotoxic profiles were determined by MTT in vitro assay against THP-1 (acute monocytic leukemia), K562 (chronic myeloid leukemia) and PBMC (peripheral blood mononuclear) human cells. To investigate the mechanism of action, cell cycle analysis and alterations of *TP53*, *p21*, *Bax*, *Bcl2*, *NOX-1*, *NOX-2*, *NOX-4* and *p47-phox* gene expressions were performed by qPCR, along with the measurement of reactive oxygen species (2',7'-dichlorodihydrofluorescein diacetate and dihydroethidium). Compounds **4c**, **5b**, **5c** and **6d** were the most active and selective for THP-1 and compounds **7c** and **11** were found to be more active for K562. All of this induced apoptosis in the tested strains. Concerning the investigation of the mechanism of action, it was observed that the pathway being activated is a p53-independent pathway. The data presented in this work indicate that 3-alkylpyridine alkaloid analogues are a potential class of compounds with cytotoxic action.

Keywords 3-alkylpyridine alkaloid analogues · Leukemia · Mode of action

Introduction

Acute Myeloid Leukemia (AML) is an aggressive malignant disease of the hematopoietic system, characterized by the uncontrolled proliferation of abnormal blastic cells of

the granulocytic lineage and the decreased production of normal blood cells (Fogliato et al. 2003; Puumala et al. 2013).

AML has abrupt clinical onset and rapid evolution to death if the patient is not treated. The aim of the treatment is to eliminate or control the proliferation of leukemic clones, and is based on the use of polychemotherapy and stem cell transplantation (Estey and Döhner 2006; Queliame et al. 2011). The gold standard treatment includes the use of cytarabine (anti-metabolic) and an anthracycline compound that causes the inhibition of topoisomerase II (daunorubicin, idarubicin or mitoxantrone) (Gong et al. 2015). However, most patients (58%) die due to a recurrence of AML (Estey and Döhner 2006).

Chronic Myelogenous Leukemia (CML) is a chronic myeloproliferative pathology arising from the clonal expansion of transformed hematopoietic stem cells, and is characterized by the presence of a specific cytogenetic abnormality, the Philadelphia (Ph) chromosome (Heiblig et al. 2014). This chromosome is a product of the t(9;22)

Supplementary information The online version of this article (<https://doi.org/10.1007/s00044-019-02395-5>) contains supplementary material, which is available to authorized users.

✉ Fernando de Pilla Varotti
varotti@ufsj.edu.br

✉ Adriano de Paula Sabino
adriansabin01@gmail.com

¹ Departamento de Análises Clínicas e Toxicológicas, Faculdade de Farmácia, Universidade Federal de Minas Gerais, Belo Horizonte, Minas Gerais, Brazil

² Núcleo de Pesquisa em Química Biológica, Universidade Federal de São João Del Rei, Divinópolis, Minas Gerais, Brazil

translocation (q34;q11) resulting in a hybrid *BCR-ABL* gene, which encodes a chimeric *BCR-ABL* oncoprotein with tyrosine kinase activity (Mughal and Goldman 2004).

The disease that was previously considered incurable now presents good results for remission and cure following the transplantation of hematopoietic stem cells. However, most patients are not able to receive this treatment, either due to old age or due to the absence of a donor (Mughal and Goldman 2004). The discovery that *BCR-ABL* is necessary for the pathogenesis of CML and that its tyrosine kinase activity is important in cell transformation has made it an important target for therapeutic intervention (Harrington et al. 2017). Thus, imatinib mesylate, which inhibits the enzymatic activity of *BCR-ABL*, has been developed, leading to the death of the leukemic cells by decreasing their resistance to apoptosis (Mahalingam et al. 2009).

The alarming increase in the number of cases and cancer deaths has boosted the search for new anti-tumor drugs. Although radiotherapy and surgery continue to be employed as first choice treatment strategies, recovery rates slightly exceed 33% (Paubelle et al. 2017).

Regarding CML, research has focused on the development of new drugs capable of combating imatinib-resistant *BCR-ABL* clones and, consequently, reducing the risk of resistance (Ramachandran et al. 2016; Egan and Radich 2016).

In this way, chemical synthesis presents itself as an important tool to obtain compounds on a larger scale and

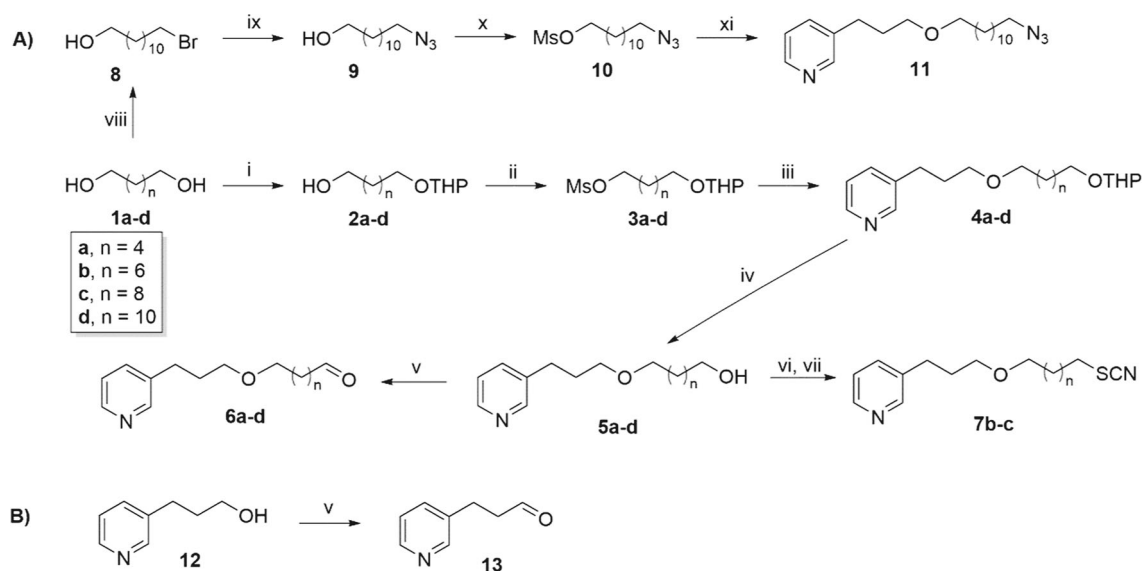
allows the investigation of the associated biological implications. It also allows modifications in the molecular architecture of analogues of natural products, which creates opportunities to obtain new bioactive compounds (Netz and Opatz 2015). In this context, synthetic analogs of alkaloids of the 3-alkylpyridine (3-APA) type are good candidates for a supposed anti-leukemic activity, since they have pro-apoptotic activity, and anti-angiogenic, anti-proliferative and cytotoxic actions against human tumoral lineages (Wang et al. 2016a; Suzuki et al. 2017). These compounds are characterized by the presence of at least one pyridine ring and a diverse functionalized aliphatic chain attached to the pyridine ring at the carbon of position 3 [15].

In view of these facts, this work aims to evaluate the mechanism of the in vitro cytotoxic action of novel synthetic molecules, 3-alkylpyridine alkaloids, against myeloid-type human leukemic cell lines.

Materials and methods

Synthesis

The synthesis of the 3-APA analogs **4a-d**, **5a-d**, **6a-d**, **7b-c**, **11** and **13** is depicted in Scheme 1. Characterization details are presented in Supporting Information. The parent nucleus of 3-alkylpyridine marine alkaloid (3-Pyridinepropanol **12**) was purchased from Sigma (cat. number: P71207).



Scheme 1 Synthesis of 3-Alkylpyridine Alkaloid Analogs **4a-d**, **5a-d**, **6a-d**, **7b-c**, **11**, **13** and the parent nucleus 3-Pyridinepropanol **12**. *Reagents, conditions, and yields:* **a** (i) NaHSO₄, DHP, DMSO, hexane, 40 °C, 16 h, 74%–89%; (ii) MsCl, Et₃N, CH₂Cl₂, r.t., 10 h, 77%–87%; (iii) 3-(pyrid-3-yl)propan-1-ol, NaOH/H₂O, Bu₄N⁺Br⁻, Et₂O, r.t., 72 h, 57%–73%; (iv) MeOH, HCl, r.t., 12 h, 71%–100%; (v) (COCl)₂,

Et₃N, DMSO, CH₂Cl₂, –60 °C, 25 min, 60–95%; (vi) MsCl, Et₃N, CH₂Cl₂, r.t. 10 h, 52%–83%; (vii) Bu₄N⁺Br⁻, KSCN, THF, reflux, 55%–78%; (viii) HBr_(aq), toluene, reflux, 69%; (ii) NaN₃, DMSO, r.t., 98%; (iii) MsCl, Et₃N, CH₂Cl₂, 100%; (iv) NaOH, Bu₄N⁺Br⁻, 63% and **b** (COCl)₂, Et₃N, DMSO, CH₂Cl₂, –60 °C, 25 min, 57%

Cell viability

The anti-leukemic activity of the synthetic compounds was evaluated by a colorimetric assay using MTT (3-(4,5-dimethylthiazol-2-yl)-2,5-diphenyltetrazolium bromide) (Sigma, St. Louis, MO, USA) (Park et al. 1987b). Cytotoxic activity was assessed in the human acute monocytic leukemia cell line THP-1 (ATCC# TIB-202), human chronic myelogenous leukemia cell line K562 (ATCC# CCL-243) and Peripheral Blood Mononuclear Cells (PBMCs). PBMCs were isolated from the peripheral blood obtained from 3 healthy individuals (The institutional Ethics Committee of Federal University of Minas Gerais approved this study, and informed consent was obtained from these control subjects) by Ficoll gradient centrifugation (Ficoll-Paque Plus, GE Healthcare Life Sciences) at room temperature. PBMC were collected, washed and resuspended in RPMI-1640 medium containing 10% of fetal bovine serum. THP-1, K562 and PBMC cells were placed in 96-well plates (1×10^6 cells per well, after cellular expansion and five maximum passages). After incubation for 24 h at 37 °C in a humidified atmosphere containing 5% CO₂, the wells were washed with the culture medium (RPMI-1640 + 20% inactivated fetal bovine serum + 2 mmol/L L-glutamine) and incubated with Control (Cytarabine—Meizler UCB Laboratories; Imatinib—EMS S/A) and compound samples at concentrations ranging from 0.10 to 250.00 µM. After 48 h of incubation, the plates were treated with MTT (5 mg/mL). All assays were performed in triplicate. The optical density (OD) of the 96-well plate contents was measured using a Spectramax plus 384 (Molecular Devices, Sunnyvale, CA, USA) spectrophotometer microplate reader at 550 nm. The OD value of formazan formed in untreated control cells was taken as 100% viability. Cytotoxicity was scored as the percent reduction in absorbance *versus* untreated control cultures (Park et al. 1987a). All experiments were performed in triplicate. The results are expressed as the mean of the IC₅₀ (the lethal drug concentration that reduced cell viability by 50%). The IC₅₀ values were calculated using OriginPro 8.0 software (OriginLab Corporation, Northampton, MA, USA). The selectivity index (SI) of the 3-APA analogs, corresponding to the ratio between the cytotoxic activities of each compound against the THP-1 and K562 cell lines and the cytotoxicity against PBMCs, was calculated as follows: $SI = IC_{50} \text{ PBMC} / IC_{50} \text{ tumor line}$.

Analysis of apoptosis/necrosis by the Annexin V/propidium iodide method

To evaluate cells in apoptosis, the Annexin V-FITC Apoptosis Detection kit (BD biosciences, cat # 556547, USA) was used following the manufacturer's instructions strictly by the flow cytometry method.

Treatments were run for 48 h in both lines, with 1×10^6 cells/tube. After the treatments, the cells were washed 2 times with phosphate buffered saline (PBS) at 4 °C and resuspended in 0.15 mL of annexin (1×) binding buffer. Cells were labeled with 50 µL of the labeling mix containing 2.5 µL annexin V-FITC and 2.5 µL IP (3 mM) and incubated for 15 min at 4 °C in the dark. Here, 20,000 events were used for cell quantification on a flow cytometer (LSR Fortessa BD biosciences). Non-stained controls were used to evaluate the autofluorescence of cells and untreated cell controls were labeled with annexin and propidium iodide to evaluate the cell death of untreated cells. The population of cells in each quadrant was determined using the software FlowJo x10.0.7 (Zhang et al. 2013).

Cell cycle analysis

The application of flow cytometry for the quantification of DNA in cell suspensions, using PI (BD biosciences, cat # 556547, USA), allows the distribution of cells in the different phases of the cell cycle, G₀/G₁, S and G₂/M, to be evaluated at any given moment; the fluorescence intensity of the IP is proportional to the amount of DNA at certain times.

For the cell cycle evaluation, 1×10^6 cells/tube were incubated with 1 mL of 70% ethanol (1 × PBS) at 4 °C for 30 min. The sample was then centrifuged (5 min at 300 × g) and resuspended in 0.2 ml PSSI solution (1.4 µl 1% Triton X-100, 20 µl RNase (20 mg), 60 µl IP 2 mg/mL, 10 mL qsp of 1 × PBS) and incubated at 4 °C for 20 min. The obtained suspension was then evaluated on the flow cytometer (LSR Fortessa BD biosciences) using an excitation wavelength of 488 nm; the filter used for the emission reading was 585/42 nm, relative to the excitation wavelengths and IP emission, with 20,000 events being evaluated in each analysis (M AWTAR KRISHAN (From the Sidney Farber Cancer Center and Harvard Medical School, Boston, Massachusetts 02115 In mammalian cell cycle studies 1975).

Gene expression analysis—Comparative real-time PCR

Total RNA was extracted with Trizol LS reagent (Invitrogen, EUA) according to the manufacturer's instructions. RNA was quantified by the Nanovue plus spectrophotometer (GE Healthcare Life Sciences) and the quality was assessed by gel electrophoresis.

Complementary DNA (cDNA) was synthesized from 1.5 µg of RNA in a total volume of 20 µL using the High-Capacity cDNA Reverse Transcription Kit, respectively (Life Technologies®, Carlsbad, California, USA).

Real-time PCR assays of the tumor suppressor protein p53 (*TP53*), cyclin-dependent kinase inhibitor 1A (*p21*),

BCL2 homologous antagonist/killer (*BAK*), B-cell lymphoma 2 (*Bcl-2*), NADPH oxidase 1 (*NOX-1*), NADPH oxidase 2 (*NOX-2*), NADPH oxidase 4 (*NOX-4*), neutrophil cytosolic factor 1 (*p47-phox*) and human glyceraldehyde-3-phosphate dehydrogenase (*GAPDH*) were carried out in duplicate in a 10 μ L volume using SYBR Green (*Thermo Fisher Scientific Inc.*, Asheville NC), and the following primers: *TP53* (5'-TGCAGCTGTGGGTTGATTCC-3')-(5-AAACACGCACCTCAAAGCTGTTC-3'); *p21* (5'-TGAGCCGCGACTGTGATG-3')-(5'-GTCTCGGTGACAAAGTCGAAGTT-3'); *BAK* (5'-TCTGGCCCTACAC-3')-(5'-ACAAACTGGCCCAACAGAAC-3'); *Bcl-2* (5'-TCCGCA TCAGGAAGGCTAGA-3')-(5'-AGGACCAGGCCTCCAAGCT-3'); *NOX-1* (5'-GCCTGTGCCCGAGCGTCTGC-3')-(5'-ACCAATGCCGTGAATCCCTAAGC-3'); *NOX-2* (5'-GGAGTTTCAAGATGCGTGGAAACTA-3')-(5'-GC CAGACTCAGAGTTGGAGATGCT-3'); *NOX-4* (5'-GT CATAAGTCATCCCTCAGA-3')-(5'-TCAGCTGAAAGACTCTTTAT-3'); *p47-phox* (5'-TTGAGAAGCGCTTCGTACCC-3')-(5'-CGTCAAACCACTTG GGAGCT-3'); and *GAPDH* (5'-GGTCGGAGTCAACGGATTG-3')-(5'-ATGAGCCCCA GCCTTCTCC AT-3'). Relative *TP53*, *p21*, *BAK*, *Bcl-2*, *NOX-1*, *NOX-2*, *NOX-4* and *p47-phox* mRNA expression levels were calculated from normalized Δ CT (cycle threshold) relative to the housekeeping gene (*GAPDH*). For the detection of changes in gene expression, normalized Δ CT values for each sample were used. The obtained values were converted to a linear scale ($2^{-\Delta\Delta CT}$) and reported as fold-change in expression (arbitrary units).

The real-time PCR assay was performed on a StepOne Real-Time PCR System (Applied Biosystems®) thermocycler under the following conditions: 95 °C for 10 min, 40 cycles of 15 s at 95 °C and 60 °C for 1 min. At the end of the process the stage of the dissociation curve is increased (95 °C for 15 s).

measurement of reactive oxygen species (ROS)

2',7'-dichlorodihydrofluorescein diacetate (H2DCFDA) and dihydroethidium (DHE) fluorescent probes were used to measure the intracellular generation of hydrogen peroxide (H₂O₂) and superoxide anions, respectively. Briefly, 1×10^6 THP-1 or K562 cells were plated in 6-well plates and allowed to attach overnight. Cells were treated or not with 3-APA analogs and then reacted with 5 μ M of H2DCF-DA or 2 μ M of DHE for 30 min at 37 °C. Cells were collected and fluorescence was analyzed by flow cytometry. The first flow cytometric analysis of cell suspension was performed in the absence of the selective fluorescence probe for reactive oxygen species to verify the basal fluorescence of blank samples. The analyses of data acquired by the flow cytometer were collected for 10,000 events.

Western blotting

THP-1 and K562 cells were washed with PBS and whole-cell extracts were prepared as previously described (Vago et al. 2012). Protein amounts were quantified with the Bradford assay reagent from Bio-Rad (Bio-Rad, Redmond, WA, USA). Extracts were separated by electrophoresis on denaturing 10% polyacrylamide-SDS gels and electrotransferred to nitrocellulose membranes, as described previously (Lima et al. 2017). Membranes were blocked for 2 h at room temperature with PBS containing 5% (w/v) nonfat dry milk and 0.1% Tween-20. After, the membranes were washed three times with PBS containing 0.1% Tween-20 and then incubated with the specific primary antibody anti-PARP (Cell Signaling Technology #9542) and normalized to anti- β -actin (Sigma #A5316) using a dilution of 1:1000 in PBS containing 5% (w/v) BSA and 0.1% Tween-20. After washing, membranes were incubated with appropriated horseradish peroxidase-conjugated secondary antibody (1:3000). Immunoreactive bands were visualized using the ECL detection system, as described by the manufacturer (GE Healthcare, Piscataway, NJ, USA). The values of cleaved PARP (89 kDa fragment) were quantified by using a densitometric analysis software (ImageJ, Image Processing and Analysis in Java; National Institutes of Health, Bethesda, MD). Changes in protein levels were estimated, and results are expressed as cleaved PARP in arbitrary units, and normalized to the values of β -actin in the same sample.

Statistical analysis

Cell viability results were expressed as the mean \pm standard deviation (Shapiro-Wilk normality test) and each experiment was performed in triplicate and repeated at least three times. The IC₅₀ values were calculated using the OriginPro 8.0 program (OriginLab Corporation, Northampton, MA, USA). The results of the gene expression were analyzed using the program "Sigma Stat" version 2.03 (Systat Software I 2013). For the data that presented normal distribution was used analysis of variance (ANOVA) followed by Tukey multiple comparison test. For those who did not present normal distribution, it was the Kruskal-Wallis non-parametric test followed by the Holm-Sidak multiple comparison test. A significant value of $p < 0.05$ was considered.

Results and discussion

Cell viability assay

In order to evaluate the in vitro cytotoxic activity of the compounds, MTT assays were performed on the human cell lines THP-1, K562 (tumor lines) and PBMC (non-tumoral),

Table 1 In vitro cytotoxic activity of new 3-APA analogs against THP-1 and K562 cell lines

Compound	THP1	IC ₅₀ (μM) ± SD*		SI	
		K562	PBMC	THP1	K562
4a	59.17 ± 5.08	88.78 ± 6.23	126.06 ± 4.64	2.13	1.42
4b	20.36 ± 2.82	28.12 ± 2.44	42.85 ± 3.57	2.10	1.52
4c	33.53 ± 2.02	49.78 ± 5.20	136.34 ± 5.10	4.06	2.73
4d	ND	92.33 ± 8.97	225.14 ± 10.55	ND	2.43
5a	ND	ND	ND	ND	ND
5b	22.11 ± 3.33	140.55 ± 4.33	192.37 ± 6.54	8.70	1.37
5c	27.19 ± 2.46	74.09 ± 8.36	215.93 ± 6.50	7.94	2.91
5d	ND	ND	246.86 ± 10.62	ND	ND
6a	59.71 ± 2.61	91.62 ± 6.69	77.10 ± 4.84	1.29	0.84
6b	48.26 ± 4.52	118.68 ± 13.70	148.61 ± 5.76	3.07	1.25
6c	85.2 ± 5.88	136.53 ± 14.61	72.21 ± 4.73	0.84	0.53
6d	37.99 ± 6.88	194.25 ± 6.90	194.63 ± 4.59	5.12	1.01
13	182.82 ± 16.87	ND	156.78 ± 10.41	0.85	1.35
7b	20.25 ± 2.82	37.71 ± 0.61	75.47 ± 5.10	3.72	2.01
7c	39.41 ± 3.77	21.66 ± 2.47	81.37 ± 9.69	2.06	3.75
11	22.06 ± 2.95	15.37 ± 2.34	48.51 ± 5.61	2.19	3.15
12	244.87 ± 6.45	217.83 ± 7.10	240.90 ± 8.05	0.98	1.10
Cytarabine	40.75 ± 4.45	81.53 ± 4.87	180.72 ± 10.45	4.43	2.21
Imatinib	ND	34.58 ± 4.2	159.34 ± 7.87	ND	4.60

*Values presented as mean ± standard deviation. *ND* Not determined. *SI* selectivity index

using cytarabine and imatinib as standard cytotoxic compounds. Table 1 shows the cytotoxicity and selectivity test data in 48 h.

It was observed that for the THP-1 line, in 48 h the compounds **4c**, **5b**, **5c** and **6d**, whose IC₅₀ values were 33.53, 22.11, 27.19, and 37.99 μM, respectively, were comparable and more selective than the standard used, cytarabine (40.75 μM), a compound which has already been used as a chemotherapeutic agent ($p < 0.05$). In the K562 line, the most effective and selective compounds were 15 (21.66 μM) and 16 (15.37 μM) ($p < 0.05$), compared to imatinib (34.58 μM). Thus, these compounds demonstrated a better cytotoxic potential compared to the cellular models studied (Table 1). The parent nucleus of 3-alkylpyridine marine alkaloid (3-Pyridinepropanol) showed no cytotoxic activity in the leukemic strains (THP-1 and K562) and PBMC (Table 1).

In an earlier study, our research group evaluated the in vitro cytotoxic potential of different 3-APA analogs in human colorectal cancer and cervical cancer cell lines and found very promising results (Gonçalves et al. 2014). Different classes of alkaloids have been described in the literature with similar in vitro cytotoxic effects in several cell lines (Gomathi and Gothandam 2016; Yao et al. 2016). However, few studies have demonstrated the cytotoxic

effects of marine alkaloids against leukemia cell lines, especially the 3-APA alkaloid (Mioso et al. 2017).

According to the observed results, it was possible to establish a relationship between the IC₅₀ values and the chemical structure of the compounds (Table 1 and Fig. 1). It is noted that with a radical change of the protecting group, such as carboxylic acid (compound **4c**), to a hydroxyl group (compounds **5b** and **5c**) or to a thiocyanate group (compounds **7c** and **11**), the biological effect increased significantly ($p < 0.05$), mainly correlating compound **4c** with the change to thiocyanate. In relation to the molecules that have a subtle difference in the chemical structure, specifically the amount of carbon in the alkyl chain, it was observed that the compounds with ten carbon atoms in the alkyl chain, compounds **5b** and **11**, had the lowest values of IC₅₀ for the two tumoral strains. In addition, compound **5b** exhibited the highest SI of the series, 8.70 for the THP-1 lineage. Compounds with a carbonyl group on the radical were also evaluated, and compound **6d**, which has five carbons in the alkyl chain, showed a significant ($p < 0.05$) increase in cytotoxic activity and SI.

Thus, compounds **4c**, **5b**, **5c**, **6d**, **7c** and **11** were shown to be strongly cytotoxic and selective for the leukemic strains and were therefore selected for evaluation of the mechanism of action.

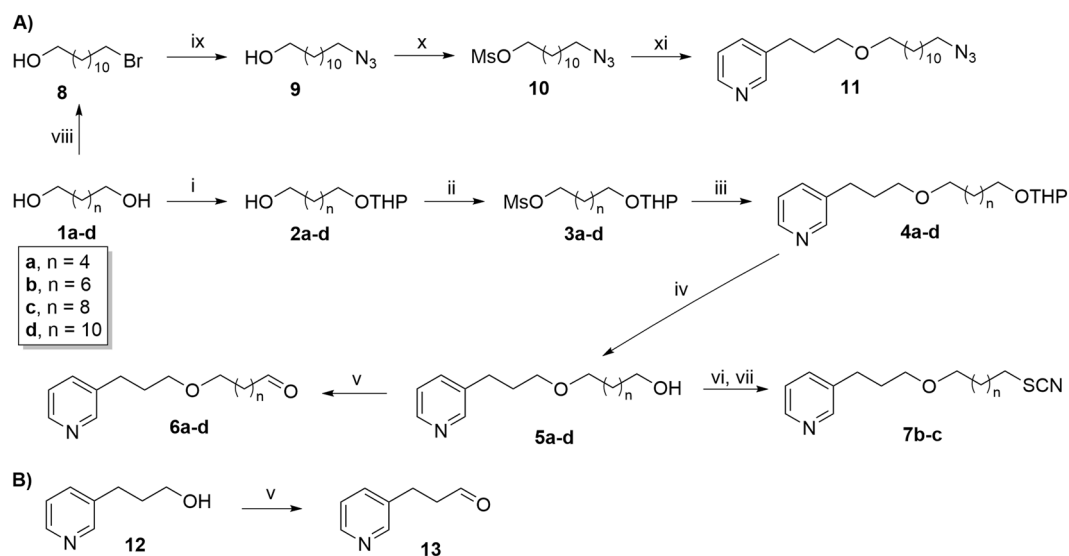


Fig. 1 Synthesis of 3-Alkylpyridine Alkaloid Analogs 4a-d, 5a-d, 6a-d, 7b-c, 11, 13 and the parent nucleus 3-Pyridinepropanol 12

Cell death induced by test compounds in leukemic cells

In order to characterize the cell death induced by the compounds, tests of Annexin-V and Propidium Iodide were performed by flow cytometry, which allowed the quantification of cells in the different stages of cell death.

After analysis of the cells by flow cytometry, a graph of the number of cells found with each type of labeling was obtained. Each of the quadrants obtained represents a different cell stage. The upper left quadrant (Q1) represents cells in necrosis, the upper right quadrant (Q2) denotes cells in late apoptosis, the lower right quadrant (Q3) represents cells in apoptosis, and the lower left quadrant (Q4) indicates viable cells. Apoptosis was the type of major cell death induced by all alkaloids (compounds **4c**, **5b**, **5c**, **6d**, **7c** and **11**) within 48 h (Fig. 1S). Clearly, approximately 50% of the cells were killed by apoptosis (treatment dose used was IC_{50}). The expressed results were considered statistically significant ($p < 0.05$) when compared with the viable cell control group (without treatment).

The results confirm that the synthetic 3-APA alkaloids induced the cells to undergo apoptosis and are therefore promising for the study of new chemotherapeutics. Other authors have also reported that different marine alkaloids induced leukemic cell apoptosis (Wang et al. 2016b; Palanisamy et al. 2017) and other tumor types (Dyshlovoy et al. 2017; Habli et al. 2017).

The Annexin V/PI assay revealed that the compounds induced apoptosis in the leukemic cells, which was further confirmed by the increased expression of *Poly(ADP-ribose) polymerase (PARP)* cleavage (Fig. 2).

Apoptosis pathway involves the activation of a family of cysteinyl-aspartate proteases (caspases). Once activated, caspases are able to cleave PARP (Pavithra et al. 2018). DNA damage promotes an increase of PARP activity (Chaitanya et al. 2010). However, caspases may inactivate PARP with apoptosis induction, impairing the ability of PARP to repair damaged DNA (Zhang et al. 2017).

Thus, to further delineate the mechanism by which compounds induced apoptosis in THP-1 and K562 cells, Western blotting assay was performed, revealing remarkably increased the PARP cleavage (Fig. 2). Several studies agree with our results, which demonstrated that the increase in PARP cleavage is linked to the induction of apoptosis through the caspase-dependent pathway (Pavithra et al. 2018).

Effect of synthetic marine alkaloids on the cell cycle

Molecular studies of carcinogenesis and apoptosis have shown that cell cycle regulation plays a role in the transformation of tumor cells and the development of resistance to chemotherapeutic agents (Schwartz and Shah 2005). These observations led to the investigation of the effect of synthetic molecules on the cell cycle in leukemic cells (Floresan et al. 2016).

Similarly, in order to elucidate a possible mechanism of action of the synthetic 3-APA alkaloids in the cell cycle, the effect of the same after 48 h of incubation with the IC_{50} concentration in different phases of the cell cycle was evaluated in this study.

In comparison to the control group, THP-1 cells treated with the compounds **5c** and **6d** induced cell cycle arrest in

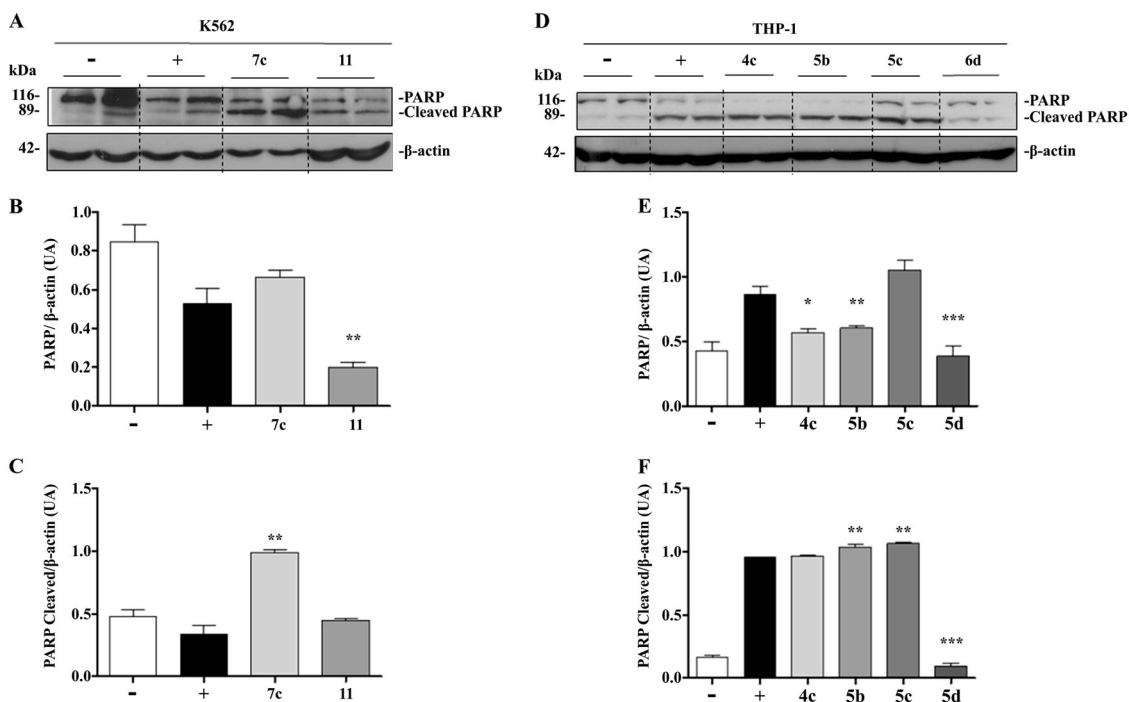


Fig. 2 Effect of compounds **4c**, **5b**, **5c**, **6d**, **7c** and **11** against K562 and THP-1 cells. THP-1 and K562 line were transferred to a 96-well plate at a density of 50,000 cells per well. Subsequently, cells were either left untreated, or treated with compounds **4c**, **5b**, **5c**, **6d**, **7c** and **11** for 48 h. **a** and **f**—PARP were assessed by western blot analysis. Blots

were normalized with β -actin and are representative of three independent experiments using pooled cells from at least four wells; **b**, **c**, **e** and **f**—Densitometry data for PARP are represented graphically. * $p < 0.05$; ** $p < 0.01$; and *** $p < 0.001$ when compared to the positive control group

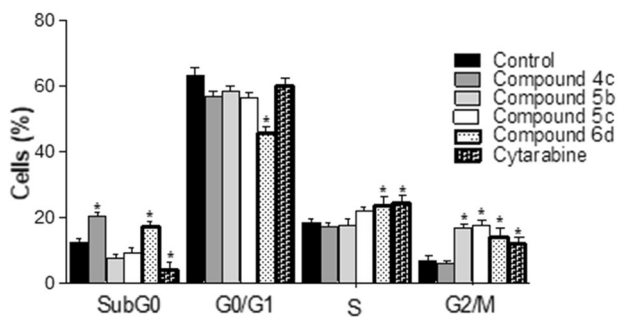


Fig. 3 Effect of 3-APA alkaloids analogues on the cell cycle against THP1 cells. THP1 cells were incubated with the alkaloids (Compounds **4c**, **5b**, **5c** and **6d**) and with cytarabine, used as a positive control. The SubG0, G0/G1, S and G2 / M phases were determined by DNA content analysis after labeling with IP and analyzed in flow cytometry. The percentage of cells in each phase was quantified by the FlowJo x10.0.7 software

the S phase (Fig. 3) and compounds **4c**, **5b**, **5c** and **6d** induced block also G2/M phase. The K562 line treated with molecules **7c** and **11** showed a similar profile to the positive control (imatinib) with a predominance in the S phase and G0/G1 (Fig. 4). The SubG0 phase corresponds to cells in apoptosis. The positive control, cytarabine, induced cell cycle arrest in the S phase, as expected, since the mechanism of action of this drug is anti-metabolic in that it

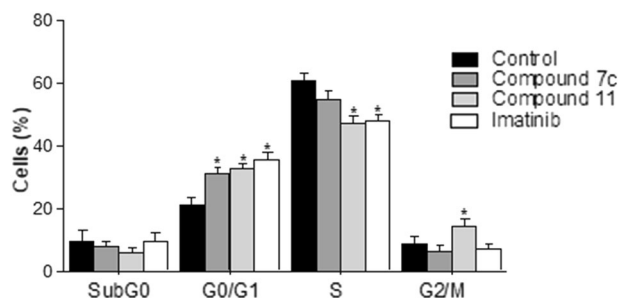


Fig. 4 Effect of 3-APA alkaloids analogues on the cell cycle against K562 cells. K562 cells were incubated with the alkaloids (Compounds **7c** and **11**) and with imatinib, used as a positive control. The SubG0, G0/G1, S and G2 / M phases were determined by DNA content analysis after labeling with IP and analyzed in flow cytometry. The percentage of cells in each phase was quantified by the FlowJo x10.0.7 software

exerts its effects mainly by blocking the S phase of the cell cycle.

The CKIs (cyclin inhibitory kinases) act by blocking CDKs and inducing cell cycle arrest. The p21, p27 and p57 proteins are important CKIs that act to inhibit cell proliferation (Wiman and Zhivotovsky 2017). From this, CKIs may be related to cell cycle arrest in G0/G1 or S seen in cell lines after incubation with the test molecules.

In THP-1 cells, proliferation blockade caused an increase in the proportion of cells in the S and G2/M phases of the cell cycle and a corresponding decrease in G0/G1 phase cells (Fig. 3). The K562 strain also had a block in the G0/G1 phase, but there was no decrease in the S phase (Fig. 4). In general, this means that progression to the S-phase of the cycle in these cell lines is prevented by the treatments.

Evaluation of gene expression by qPCR

In order to determine which signaling pathway was activated in apoptosis in the leukemic cells treated with the selected compounds, gene expression analysis of genes involved in this pathway was performed by a quantitative PCR assay. In Figs. 5, 6, the relative expressions of each target gene relative to the control cells (considered as 1.0) are shown, using *GAPDH* as the normalizing gene.

A common feature in many tumor cells is the presence of the *TP53* gene. However, in many leukemia cell lines, the lack of expression of the *TP53* gene is identified (Benton and Ravandi 2017). The mechanism responsible for the silencing of this gene in myeloid tumors remains unknown. The p53 protein is an important cell transcription factor involved in the induction of apoptosis (activation of the *Bax* gene, whose protein inhibits the anti-apoptotic action of the Bcl-2 protein) and also in the activation of the p21 protein, which results in the G1 phase of the cell cycle being stopped (Dyshlovoy et al. 2017).

The cellular response to DNA damage involves the transcription of the *TP53* gene, which is responsible for the induction of the G1/S checkpoint of mitosis and pro-apoptotic molecules. However, THP-1 and K562 cell lines show a deficiency in *TP53* expression (Figs. 5, 6) (Hu et al. 2013). In leukemia models, the detection of mutations and chromosomal deletions at this locus is associated with partial or total resistance to treatment both in vitro and in vivo (Yao et al. 2016; Benton and Ravandi 2017). In this sense, treatment should be focused on p53-independent pathways.

Thus, the absence of *TP53* expression observed 48 h after exposure to treatments was expected. There was also only a slight or no change in the expression of all other target genes (*p21*, *Bak* and *Bcl2*) after 48 h (Figs. 5, 6).

For *Bak* levels, no significant difference was observed in relation to the control cells in any of the treatments (Figs. 5, 6). *Bak*, a key pro-apoptotic signaling regulator, showed elevated levels related to tumor suppression in an apoptotic p53-independent pathway. However, in some studies, the low expression of *Bak* was able to induce apoptosis by activating caspase 3 in gastric cancer cells in vitro in a p53-independent pathway (Kubo et al. 2015).

In addition, these alkaloids either decreased or did not alter *Bcl-2* expression, which suggests that upon initiation

of the apoptosis signal, the anti-apoptotic proteins involved are inhibited; however, if the inhibition signal does not persist, they are expressed.

The compounds also induced a strong decrease in p21 expression. The p21 protein is a kinase-dependent cyclin inhibitory protein, which participates in cell cycle regulation, and acts by inducing cell cycle arrest (Schwartz and Shah 2005; Kumar et al. 2015; Wiman and Zhivotovsky 2017). However, the p21 protein may also act in an anti-apoptotic manner by inhibiting caspase-3 cleavage and inhibiting the stress pathways JNK1/SAPK and MAPK ASK1/MEKK5 (Kumar et al. 2015). Additionally, a high expression of the p21 protein in the cytoplasm could lead the cells to become resistant to apoptosis (Shen et al. 2007). Our results demonstrate that compounds **4c**, **6d**, **7c** and **11** induced a reduction or non-alteration of *p21* expression at 48 h, possibly thus facilitating the activation of caspase-3 and consequently apoptosis (Figs. 5, 6). Compounds **5b** and **5c**, however, showed a statistically significant increase in the expression of *p21* with the IC₅₀ concentration in 48 h (Figs. 5, 6).

In general, a dose-response relationship was noted between the expressions at the same treatment time, in which some discrepancies in the expression at the IC₅₀ concentration were noted (Figs. 5, 6).

These data suggest that the compounds induce a p53-independent pathway to activate apoptosis, showing that these complexes possibly interfere with DNA replication, probably by interacting directly with DNA. These in vitro results suggest that the compounds are a potential prototype of a DNA-damaging anticancer agent against AML and CML. Other studies suggest that alkaloid derivatives have a cytotoxic effect on cancer cells regardless of p53 status (Benton and Ravandi 2017).

Most of the conventional anticancer drugs induce cell death, with the main focus of action being the induction of cellular stress and DNA lesions (Mahalingam et al. 2009). Thus, to date, the data presented in this work indicate that 3-alkylpyridine alkaloid analogues are a potential class of compounds with cytotoxic action in vitro, showing DNA damage through the activation of apoptosis via the p53-independent pathway. Thus, the investigation of the induction of apoptosis, for example via Reactive oxygen species (ROS), becomes interesting to explain the mechanism of action of the test molecules. Facing this scenario, the screening of new compounds becomes an extremely complex and challenging but indispensable task.

Analysis of ROS

ROS can induce proliferation, apoptosis, and gene expression changes (Zhang et al. 2017). Cytotoxic drugs used in leukemia therapy has as mechanism of action the alteration

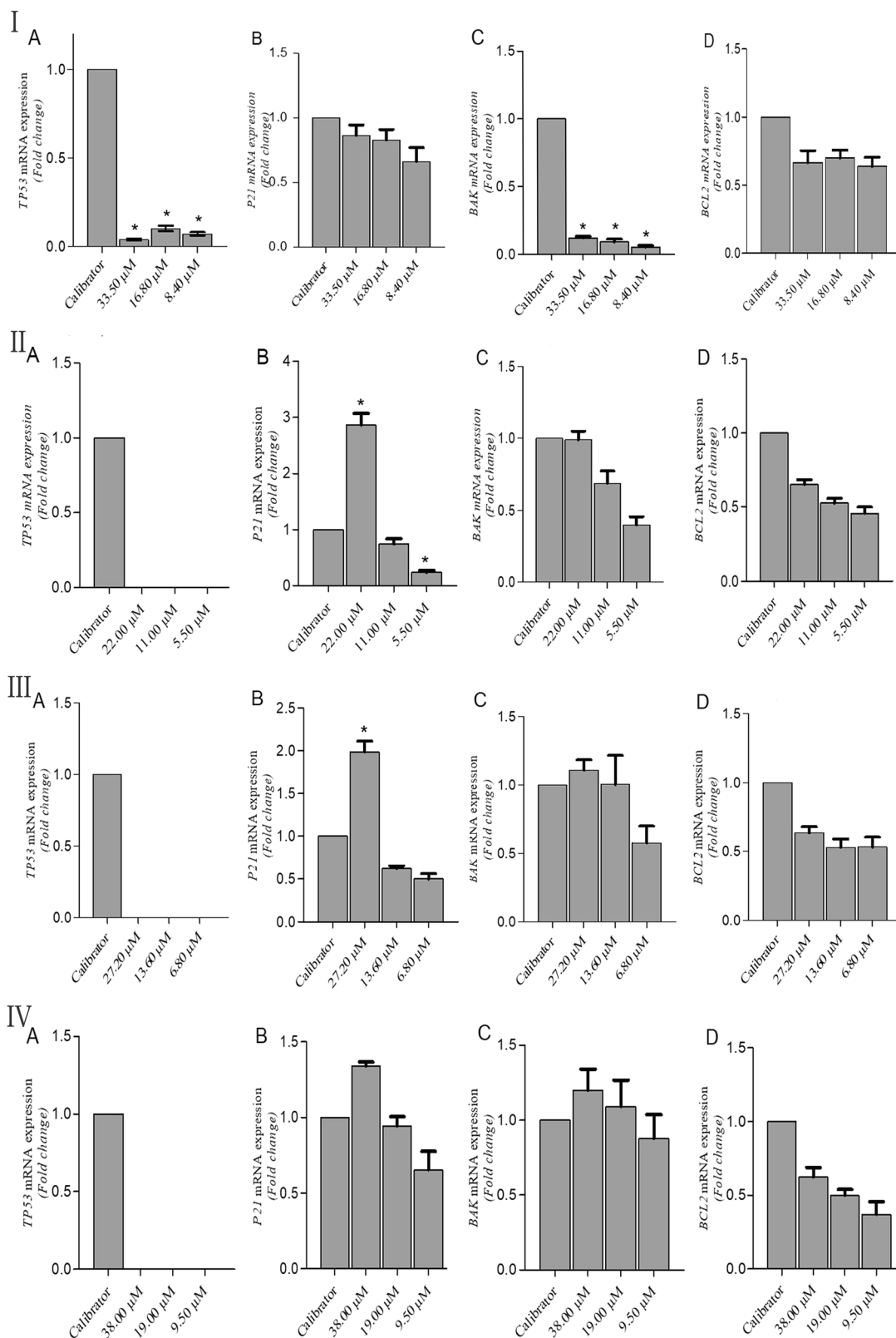


Fig. 5 Effects of the compounds **4c**(I), **5b**(II), **5c**(III) and **6d** (IV) on the expression of target genes against THP-1 cell line. **a** Relative quantification of the *TP53* gene, **b** *p21*, **c** *Bak* and (**#**) *Bcl2*. Cells (1×10^6) were incubated with compound **4c** for 48 h. Each bar represents

the mean \pm standard deviation ($n = 3$) of relative quantification. The data were expressed in relation to the control of cells without treatment considered as 1. Value of $*p < 0.05$ was considered statistically significant when compared to the control without treatment

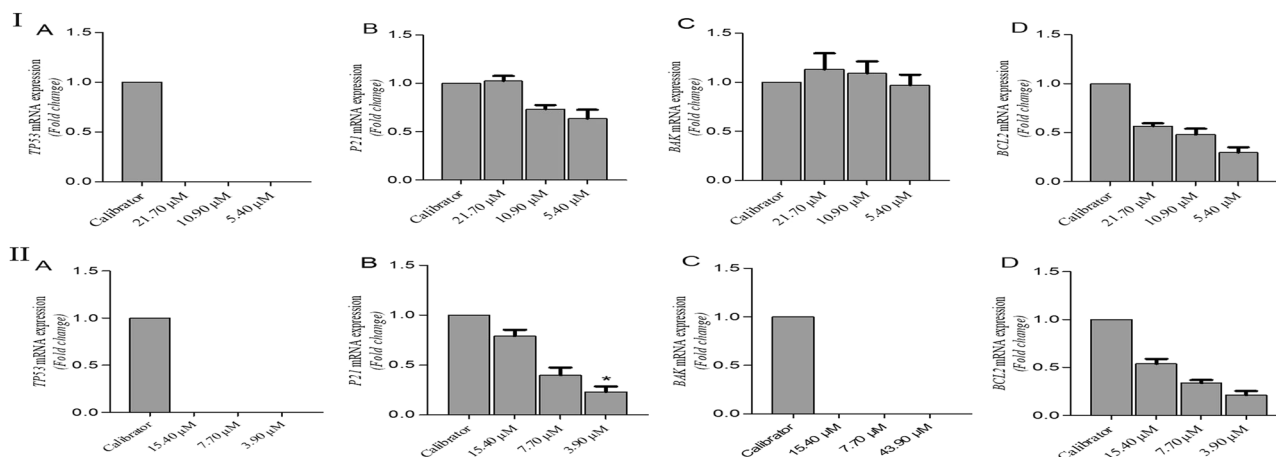


Fig. 6 Effect of the compounds **7c**(I) and **11**(II) on the expression of target genes against K562 cell line. **a** Relative quantification of the *TP53* gene, **b** *p21*, **c** *Bak* and **d** *Bcl2*. Cells (1×10^6) were incubated with the compound **7c** for 48 h. Each bar represents the mean \pm

standard deviation ($n = 3$) of relative quantification. The data were expressed in relation to the control of cells without treatment considered as 1. Value of $*p < 0.05$ was considered statistically significant when compared to the control without treatment

of the DNA replication process of the malignant cells (Antoszewska-smith et al. 2017). Oxidants compounds are used for the treatment of hematological malignancies, despite their negative effects (Chen et al. 2017). An increase in ROS can induce cell death, lipid peroxidation, protein oxidation and mutation, increased mitochondrial stress and apoptosis, and activation of a G2/M phase cell cycle checkpoint (Chen et al. 2017).

Pro-oxidant treatment and malignant cells can cause depletion of antioxidant defenses, inducing increased production of ROS (Trachootham et al. 2009). However, if oxidative species are duplicated by the treatment action, malignant cells may become sensitized and prolong treatment or activate the apoptosis pathway (Al. HDH et 2008).

ROS can induce damage to the genetic material and oxidize proteins and lipids, leading to cell death (Liu et al. 2016). Various ROS-generating drugs have proven to be effective in cancer, due to its action of provoking an increase in ROS levels, which causes damage to cellular components and the activation of cellular signaling pathways (Chen et al. 2017).

Many antitumor agents, such as vinblastine, cisplatin, mitomycin C, doxorubicin, camptothecin and neocarzinostatin, exhibit antitumor activity through the activation of ROS-dependent apoptotic cell death, suggesting the potential use of ROS as a cytotoxic agent (Chen et al. 2017). Thus, an anticancer strategy called “oxidation therapy” was developed by the induction of cytotoxic oxidative stress for the treatment of cancer.

The basal fluorescence intensity emitted by H2DCFDA and DHE cell lines treated with the compounds was increased when compared to the control (Fig. 2S). In both

cells lines, there was a significant increase in the DHE marker in relation to the negative control (no-treatment). In the case of H2DCFDA, there was a significant increase in the level of ROS in THP-1 and K562, compared to the negative control, while for molecule **7c**, there was an increase, but it was not significant (Fig. 2S). All analogous molecules of alkaloids of the 3-alkylpyridine showed levels of ROS which were similar to or even greater than the positive control (phorbol myristate acetate) and the traditional drug (cytarabine and imatinib).

Main ROS are generated by the NOX family of NADPH oxidases (NOX) which are regulatory molecules cell growth and migration (Liu et al. 2016). The three NOX homologues, namely NOX1, NOX2 and NOX4, have been identified in mammalian cells (Chen et al. 2017) and the p47phox is a cytosolic regulatory subunit of NOX (Antoszewska-smith et al. 2017).

Each NADPH oxidase seems to have a particular pattern of expression, and most cells express different members of this family. The importance of these enzymes in cancer is beginning to be recognized and, interestingly, it has recently been shown that NADPH oxidase inhibitors are efficient at preventing the growth of cancer. This suggests that NADPH oxidases could be exploited as therapeutic targets in the cancer treatment setting.

Therefore, the genetic expression of *NOX1*, *NOX2*, *NOX4* and p47^{phox} is shown in Figs. 3S, 4S.

In the THP-1 line, there was a significant increase in the calibration of *NOX-1* (5b, 5c and cytarabine), *NOX-2* (5b, 5c, 6d and cytarabine), *NOX-4* (4c, 5b, 6d and cytarabine) and p47^{phox} (4c, 5b, 5c, 6d and cytarabine) (Fig. 3S). In the K562 line, a significant increase in gene expression was

observed for the *NOX-1* (7c, 11 and imatinib), *NOX-2* (11 and imatinib), *NOX-4* (7c and 11) and *p47^{phox}* (7c, 11 and imatinib) genes (Fig. 4S).

In this way, the increase in oxidative stress in cells produce oxidized lipids, proteins, and damaged DNA, which would consequently lead to cell death. Thus, the analogous molecules of alkaloids of the 3-alkylpyridine are in some way inducing the production of ROS, thereby causing DNA damage, which contributes to the cytotoxic mechanism of these compounds.

Conclusions

Our study shows that the selected compounds induced apoptosis and it was observed that the pathway being activated is independent of p53. Overall, the data presented in this work indicate that 3-alkylpyridine alkaloid analogues are a potential class of compounds with cytotoxic action *in vitro*.

Acknowledgements The authors are grateful to Conselho Nacional de Desenvolvimento Científico e Tecnológico (CNPq), Fundação de Amparo à Pesquisa do Estado de Minas Gerais (FAPEMIG), Coordenação de Aperfeiçoamento de Pessoal de Nível Superior (CAPES) and Pro-Reitoria de Pesquisa (PRPq) da Universidade Federal de Minas Gerais, for sponsoring this study.

Compliance with ethical standards

Conflict of interest The authors declare that they have no conflict of interest.

Publisher's note: Springer Nature remains neutral with regard to jurisdictional claims in published maps and institutional affiliations.

References

- Halicka D, Ita M, Tanaka T, Kurose A, Darzynkiewicz Z (2008) Biscoclaurine alkaloid cepharanthine protects DNA in TK6 lymphoblastoid cells from constitutive oxidative damage. *Pharmacol Rep* 60:93–100
- Antoszevska-smith J, Pawlowska E, Blasiak J (2017) Reactive oxygen species in BCR-ABL1-expressing cells—relevance to chronic myeloid leukemia. *Acta Biochim Pol* 64:1–10. https://doi.org/10.18388/abp.2016_1396
- Benton CB, Ravandi F (2017) Targeting acute myeloid leukemia with TP53-independent vosaroxin. *Future Oncol* 13:125–133
- Chaitanya GV, Alexander JS, Babu PP (2010) PARP-1 cleavage fragments: Signatures of cell-death proteases in neurodegeneration. *Cell Commun Signal* 8:31. <https://doi.org/10.1186/1478-811X-8-31>
- Chen Y-F, Liu H, Luo X-J et al. (2017) The roles of reactive oxygen species (ROS) and autophagy in the survival and death of leukemia cells. *Crit Rev Oncol Hematol* 112:21–30. <https://doi.org/10.1016/j.critrevonc.2017.02.004>
- Dyshlovoy SA, Madanchi R, Hauschild J et al. (2017) The marine triterpene glycoside frondoside A induces p53-independent apoptosis and inhibits autophagy in urothelial carcinoma cells. *BMC Cancer* 17:93. <https://doi.org/10.1186/s12885-017-3085-z>
- Egan D, Radich J (2016) Making the diagnosis, the tools, and risk stratification: More than just BCR-ABL. *Best Pr Res Clin Haematol* 29:252–263. <https://doi.org/10.1016/j.beha.2016.10.015>
- Estey E, Döhner H (2006) Acute myeloid leukaemia. *Lancet* 368:1894–1907. [https://doi.org/10.1016/S0140-6736\(06\)69780-8](https://doi.org/10.1016/S0140-6736(06)69780-8)
- Floresan C, Schneckeburger M, Lee J-Y et al. (2016) Discovery and characterization of Isofistularin-3, a marine brominated alkaloid, as a new DNA demethylating agent inducing cell cycle arrest and sensitization to TRAIL in cancer cells. *Oncotarget* 7:24027–24049. <https://doi.org/10.18632/oncotarget.8210>
- Fogliato L, Daudt L, Bittencourt HNS, Cruz MS (2003) Leucemia Mielóide Aguda: perfil de duas décadas do Serviço de Hematologia do Hospital de Clínicas de Porto Alegre—RS Acute Myelogenous Leukemia: two decades overview—Hematology Service. *Rev Bras Hematol Hemotr* 25:17–24. <https://doi.org/10.1590/S1516-84842003000100004>
- Gomathi A, Gothandam KM (2016) Ocean dwelling actinobacteria as source of antitumor compounds. *Braz Arch Biol Technol* 59:1–21
- Gonçalves AMMN, De Lima AB, Da Silva Barbosa MC et al. (2014) Synthesis and biological evaluation of novel 3-alkylpyridine marine alkaloid analogs with promising anticancer activity. *Mar Drugs* 12:4361–4378. <https://doi.org/10.3390/md12084361>
- Gong Q, Zhou L, Xu S et al. (2015) High doses of daunorubicin during induction therapy of newly diagnosed acute myeloid leukemia: A systematic review and meta-analysis of prospective clinical trials. *PLoS One* 10:1–14. <https://doi.org/10.1371/journal.pone.0125612>
- Habli Z, Toumieh G, Fatfat M et al. (2017) Emerging cytotoxic alkaloids in the battle against cancer: overview of molecular mechanisms. *Molecules* 22:250. <https://doi.org/10.3390/molecules22020250>
- Harrington P, Kizilors A, de Lavallade H (2017) The role of early molecular response in the management of chronic phase CML. *Curr Hematol Malig Rep*. <https://doi.org/10.1007/s11899-017-0375-0>
- Heiblig M, Sobh M, Nicolini FE (2014) Subcutaneous omacetaxine mepesuccinate in patients with chronic myeloid leukemia in tyrosine kinase inhibitor-resistant patients: Review and perspectives. *Leuk Res* 38:1145–1153. <https://doi.org/10.1016/j.leukres.2014.05.007>
- Hu W, Ge Y, Ojcius DM et al. (2013) P53 signalling controls cell cycle arrest and caspase-independent apoptosis in macrophages infected with pathogenic leptospira species. *Cell Microbiol* 15:1624–1659. <https://doi.org/10.1111/emi.12141>
- Kubo T, Kawano Y, Himuro N et al. (2015) BAK is a predictive and prognostic biomarker for the therapeutic effect of docetaxel treatment in patients with advanced gastric cancer. *Gastric Cancer* 19:827–838. <https://doi.org/10.1007/s10120-015-0557-1>
- Kumar S, Guru SK, Pathania AS et al. (2015) Fascaplysin induces caspase mediated crosstalk between apoptosis and autophagy through the inhibition of PI3K/AKT/mTOR signaling cascade in human leukemia HL-60 cells. *J Cell Biochem* 116:985–997. <https://doi.org/10.1002/jcb.25053>
- Lima KM, Vago JP, Caux TR et al. (2017) The resolution of acute inflammation induced by cyclic AMP is dependent on annexin A1. *J Biol Chem* 292:13758–13773. <https://doi.org/10.1074/jbc.M117.800391>
- Liu G-Y, Zhai Q, Chen J-Z et al. (2016) 2,2'-Fluorine mono-carbonyl curcumin induce reactive oxygen species-Mediated apoptosis in Human lung cancer NCI-H460 cells. *Eur J Pharm* 786:161–168. <https://doi.org/10.1016/J.EJPHAR.2016.06.009>
- Krishan, A (From the Sidney Farber Cancer Center and Harvard Medical School, Boston, Massachusetts 02115 In mammalian cell cycle studies OO (1975) Rapid flow cytofluorometric mammalian analysis of iodide staining. *Cell Cycle* 66:188–93

- Mahalingam D, Swords R, Carew JS et al. (2009) Targeting HSP90 for cancer therapy. *Br J Cancer* 100:1523–1529. <https://doi.org/10.1038/sj.bjc.6605066>
- Mioso R, Marante F, Bezerra R et al. (2017) Cytotoxic compounds derived from marine sponges: a review (2010–2012). *Molecules* 22:208. <https://doi.org/10.3390/molecules22020208>
- Mughal TI, Goldman JM (2004) Chronic myeloid leukemia: current status and controversies. *Oncology* 18:837–844, 847; 847-50:853–854
- Netz N, Opatz T (2015) Marine indole alkaloids. *Mar Drugs* 13:4814–4914. <https://doi.org/10.3390/md13084814>
- Palanisamy SK, Rajendran NM, Marino A (2017) Natural products diversity of marine Ascidiaceae (Tunicates; Ascidiacea) and successful drugs in clinical development. *Nat Prod Bioprospect* 7:1–111. <https://doi.org/10.1007/s13659-016-0115-5>
- Park JG, Kramer BS, Steinberg SM, et al. (1987a) Chemosensitivity testing of human colorectal carcinoma cell lines using a tetrazolium-based colorimetric assay. *Cancer Res* 47:5875–5879
- Park KS, Frost B, Tuck M et al. (1987b) Enzymatic methylation of in vitro synthesized apocytocrome c enhances its transport into mitochondria. *J Biol Chem* 262:14702–14708
- Paubelle E, Zylbersztejn F, Thomas X (2017) The preclinical discovery of vosaroxin for the treatment of acute myeloid leukemia. *Expert Opin Drug Discov*. <https://doi.org/10.1080/17460441.2017.1331215>
- Pavithra PS, Mehta A, Verma RS (2018) Aromadendrene oxide 2, induces apoptosis in skin epidermoid cancer cells through ROS mediated mitochondrial pathway. *Life Sci* 197:19–29. <https://doi.org/10.1016/j.lfs.2018.01.029>
- Puumala SE, Ross Ja, Aplenc R, Spector LG (2013) Epidemiology of childhood acute myeloid leukemia. *Pedia Blood Cancer* 60:728–733. <https://doi.org/10.1002/pbc.24464>
- Queliane Carvalho S, Pedrosa A, Sebastião P (2011) Leucemia mieloide aguda versus ocupação profissional: perfil dos trabalhadores atendidos no Hospital de Hematologia de Recife *. *Rev Esc Enferm USP* 45:1446
- Ramachandran KC, Narayanan G, Nair SG et al. (2016) Isodicentric Philadelphia chromosome: a rare chromosomal aberration in imatinib-resistant chronic myelogenous leukemia patients—case report with review of the literature. *Cytogenet Genome Res* 150:273–280. <https://doi.org/10.1159/000458164>
- Schwartz GK, Shah MA (2005) Targeting the cell cycle: a new approach to cancer therapy. *J Clin Oncol* 23:9408–9421. <https://doi.org/10.1200/JCO.2005.01.5594>
- Shen K-H, Chang J-K, Hsu Y-L, Kuo P-L (2007) Chalcone arrests cell cycle progression and induces apoptosis through induction of mitochondrial pathway and inhibition of nuclear factor kappa B signalling in human bladder cancer cells. *Basic Clin Pharm Toxicol* 101:254–261. <https://doi.org/10.1111/j.1742-7843.2007.00120.x>
- Suzuki Y, Saito Y, Goto M et al. (2017) Neocaryachine, an anti-proliferative piperidine alkaloid from *Cryptocarya laevigata*, induces DNA double-strand breaks. *J Nat Prod* 80:220–224. <https://doi.org/10.1021/acs.jnatprod.6b01153>
- Systat Software I (2013) Sigma Stat versão 2.03. <https://systatsoftware.com/products/sigmaplot/>. Accessed 14 May 2017
- Trachootham D, Alexandre J, Huang P (2009) Targeting cancer cells by ROS-mediated mechanisms: a radical therapeutic approach? *Nat Rev Drug Discov* 8:579–591. <https://doi.org/10.1038/nrd2803>
- Vago JP, Nogueira CRC, Tavares LP et al. (2012) Annexin A1 modulates natural and glucocorticoid-induced resolution of inflammation by enhancing neutrophil apoptosis. *J Leukoc Biol* 92:249–258. <https://doi.org/10.1189/jlb.0112008>
- Wang X-D, Li C-Y, Jiang M-M et al. (2016a) Induction of apoptosis in human leukemia cells through an intrinsic pathway by cathaechunine, a unique alkaloid isolated from *Catharanthus roseus*. *Phytomedicine* 23:641–653. <https://doi.org/10.1016/j.phymed.2016.03.003>
- Wang XD, Li CY, Jiang MM et al. (2016b) Induction of apoptosis in human leukemia cells through an intrinsic pathway by cathaechunine, a unique alkaloid isolated from *Catharanthus roseus*. *Phytomedicine* 23:641–653. <https://doi.org/10.1016/j.phymed.2016.03.003>
- Wiman KG, Zhivotovsky B (2017) Understanding cell cycle and cell death regulation provides novel weapons against human diseases. *J Intern Med*. <https://doi.org/10.1111/joim.12609>
- Yao J, Jiao R, Liu C et al. (2016) Assessment of the cytotoxic and apoptotic effects of chaetominine in a human leukemia cell line. *Biomol Ther* 24:147–155. <https://doi.org/10.4062/biomolther.2015.093>
- Zhang J, Fu X-L, Yang N, Wang Q-A (2013) Synthesis and cytotoxicity of chalcones and 5-deoxyflavonoids. *Sci World J* 2013:649485. <https://doi.org/10.1155/2013/649485>
- Zhang J, Wang Y, Zhou Y, He Q (2017) Jolkinolide B induces apoptosis of colorectal carcinoma through ROS-ER stress-Ca²⁺-mitochondria dependent pathway. *Oncotarget* 8:91223–91237. <https://doi.org/10.18632/oncotarget.20077>